

Self-mixing interferometer based on sinusoidal phase modulating technique

Dongmei Guo, Ming Wang* and Suqing Tan

Department of Physics, Nanjing Normal University, Nanjing 210097, P. R. China
wangming@njnu.edu.cn

Abstract: A new self-mixing interferometry based on sinusoidal phase modulating technique is presented. Self-mixing interference occurs in the laser cavity by reflecting the light from a mirror-like target in front of the laser. Sinusoidal phase modulation of the beam is obtained by an electro-optic modulator (EOM) in the external cavity. The phase of the interference signal is calculated by Fourier analysis method. The interferometer is applied to measure the displacement of a high-precision commercial PZT with an accuracy of <10nm. The measurement range of the system mainly depends on the maximum operating frequency of EOM and the maximum sampling rate of A/D converter.

©2005 Optical Society of America

OCIS codes: (120.3180) Interferometry; (120.5050) Phase measurement; (120.5060) Phase modulation;

References and links

1. Th. H. Peek, P. T. Bolwjin, and C. Th. Alkemade, "Axial mode number of gas lasers from moving-mirror experiments," *Am. J. Phys.* **35**, 820-831 (1967).
2. T. Yoshino, M. Nara, S. Mnatzakanian, "Laser diode feedback interferometer for stabilization and displacement measurements," *Appl Opt.* **26**, 872-877 (1987).
3. S. Shinohara, A. Mochizuki, H. Yoshida et al. "Laser Doppler velocimeter using the self-mixing effect of a semiconductor laser diode," *Appl Opt.* **25**, 1417-1419 (1986).
4. S. Shinohara, H. Yoshida, H. Ikeda, K. Nishide, and M. Sumi, "Compact and high-precision range finder with wide dynamic range and its application," *IEEE Trans Instrum. Meas.* **41**, 40-44 (1992).
5. Kato J, Kikuchi N, Yamaguchi I, Ozono S. "Optical feedback displacement sensor using a laser diode and its performance improvement," *Meas. Sci. Technol.* **6**, 45-52 (1995).
6. T. Suzuki, S. Hirabayashi, O. Sasaki et al "Self-mixing type of phase-locked laser diode interferometry," *Opt. Eng.* **38**, 543-548 (1999).
7. M. Wang, Guangming Lai, "Displacement measurement based on Fourier transform method with external cavity modulation," *Rev. Sci. Instrum.* **72**, 3440-3445 (2001).
8. B. Ovryn, J. H. Andrews, "Phase-shifted laser feedback interferometry," *Opt. Lett.* **23**, 1078-1080 (1998).
9. G. Liu, S. L. Zhang et al, "Theoretical and experimental study of intensity branch phenomena in self-mixing interference in a He-Ne laser," *Opt. Commun.* **221**, 387-393 (2003).

1. Introduction

Self-mixing interferometer (SMI) demonstrates unique features since it was first reported in the 1960's to measure changes in the optical length (OPL) and the behavior of lasers [1]. These features include a simple, single-axis optical arrangement that requires minimal optical components and high sensitivity at low light level. SMI has been widely used for displacement, velocity measurement and ranging [2-4].

SMI was used to measure displacement with an accuracy of $\lambda/2$ by counting interference signal peaks. In order to increase the measurement accuracy beyond $\lambda/2$, some methods for analysis of SMI signal have been reported. J. Kato et al measured displacement by calculating

the ratio of a phase shift and a period based on pseudo-heterodyne method [5]. The phase-locked technique was introduced in the SMI using a feedback loop [6]. The double external cavity method combined with FFT technique was reported to improve the displacement measurement accuracy [7]. Ovrn et al. used the phase shifting technique in the external cavity to analyze the SMI signal [8].

In this article a new self-mixing interferometry based on sinusoidal phase modulating technique is proposed. An EOM situated in the beam path between the front mirror of the laser and the external target is used to introduce phase modulation in the OPL. Considering that the characteristic of a He-Ne laser beam is quite better than that of a semiconductor laser and the polarization characteristic which is appropriate for EOM, we use a linearly polarized He-Ne laser as the coherent source. Fourier analysis method is proposed to extract phase from the modulated interference signal. Theoretical analysis and simulation results are presented. The optimum range of the modulation depth and the modulation frequency are discussed. Experimentally, the movement of a high-precision commercial PZT is reconstructed and a displacement measurement accuracy of <10nm can be obtained.

2. Experimental setup

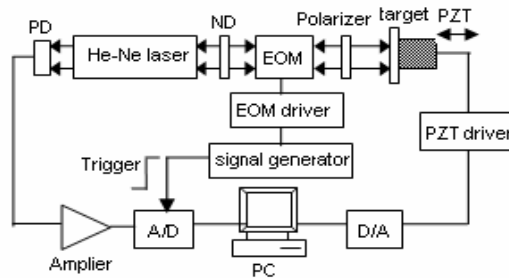


Fig. 1. Experimental setup.

The experimental setup is shown in Fig. 1. The light source is a 1mW linearly polarized He-Ne (632.8nm, TEM₀₀) laser. The laser cavity consists of a plane mirror (front mirror) and a concave mirror (back mirror) which has a radius of 1m. Their reflectivities are 0.98 and 0.99 respectively. The reflectivity of the external target is 0.04. The length of the laser cavity and the external cavity are 180mm and 200mm, respectively. The beam emitted from the front mirror of the laser is sent through a various neutral density (ND) filter, an EOM (New Focus, 4002), a linear polarizer with a fixed orientation parallel to the polarization of the laser and then reflected back to the laser cavity by the external target. The interference signal is monitored by a photodiode (PD) situated behind the back mirror of the laser. The angle between the polarization direction of the laser and the electro-optically active axis of EOM is 0°. Then the EOM can provide pure phase modulation with extremely low amplitude modulation. The Brewster window in the laser cavity and the linear polarizer in the external cavity make the interferometer more immune to a little change in the polarization of the laser beam caused by EOM. The external target is fixed on a high-precision commercial PZT (PI, P-841.10) which can obtain displacement accuracy of 0.15nm based on the close-loop design. The voltage signal from the PD is amplified and then digitized with a 200-KHZ, 12-bit analog-to-digital board on a PC bus (National Instrument, NI 6024E); this board is also used to send voltage to the PZT driver.

3. Theoretical analysis and simulation results

The basic theory of a He-Ne laser SMI can be explained by a three-mirror cavity model. The light emitted from the laser is reflected from the external target, a portion of the laser output back into the laser cavity and mix with the original light in the laser cavity forming the self-mixing effect. We assume that the laser's frequency is unperturbed by the optical feedback. This assumption is appropriate for gas lasers with symmetric gain and dispersion curves. The output intensity of a He-Ne laser SMI can be expressed as [8-9]

$$I = I_0 \left[1 + m \cos(\phi) \sum_{j=0}^{\infty} (-\eta)^j \cos(j\phi) \right] \quad (1)$$

Where $\phi = 4\pi L / \lambda$, $m = K\eta / l$, I_0 is the power of the laser output without feedback, η is the parameter denoting coupling effect from the external cavity back into the laser cavity, l is the length of the laser cavity, L is the length of the external cavity, λ is the wavelength of the laser, K is a constant relating to the laser's operating parameters. Also included in Eq. (1) is the effect of multiple reflections that can occur between the external target and the laser's output mirror. Clearly, m/η has no relation with the optical feedback.

Assuming that SMI operates in a low-feedback regime where the effect of multiple reflections in the external cavity is small (i.e., η is small), Eq. (1) can be expressed as

$$I = I_0 [1 + m \cos(\phi)] \quad (2)$$

This assumption forms the basis of our subsequent research. Error caused by multiple reflections will be considered later. Using this simple configuration, the displacement of the external target can be measured by counting interference signal peaks. To achieve higher accuracy, an experimentally controlled additive phase $\psi(t) = a \sin(2\pi f_m t + \beta)$ is introduced by EOM situated in the external cavity, where a is the modulation depth, f_m is the modulation frequency, β is the initial phase of the modulation. Considering that the beam pass through the EOM twice in the external cavity, the modulated interference signal can be written as

$$I(t) = I_0 \{1 + m \cos[\phi(t) + 2a \sin(2\pi f_m t + \beta)]\} \quad (3)$$

Expanding Eq. (3) in a Fourier series, harmonics at frequency f_m and $2f_m$ have following expressions:

$$\begin{aligned} I(f_m, t) &= -2mI_0 \sin \phi(t) J_1(2a) \sin(2\pi f_m t + \beta) \\ &= A_1(t) \sin(2\pi f_m t + \beta) \end{aligned} \quad (4)$$

$$\begin{aligned} I(2f_m, t) &= -2mI_0 \cos \phi(t) J_2(2a) \cos(4\pi f_m t + 2\beta) \\ &= A_2(t) \cos(4\pi f_m t + 2\beta) \end{aligned} \quad (5)$$

Where $J_n(2a)$ is the n th-order Bessel function. Then we can calculate the phase $\phi(t)$ from $A_1(t)$ and $A_2(t)$ using the subsequent relation:

$$\phi(t) = \arctan \left[\frac{A_1(t)}{A_2(t)} \cdot \frac{J_2(2a)}{J_1(2a)} \right] \quad (6)$$

The Fourier analysis method is proposed to determine the values of $A_1(t)$ and $A_2(t)$. It mainly takes following steps: (1) taking the Fourier transform of the interference signal; (2) selecting the first harmonic $I(f_m)$ and second harmonic components $I(2f_m)$ of the Fourier spectra with two windows: $f_m/2 < f < 3f_m/2$ and $3f_m/2 < f < 5f_m/2$; (3) taking the inverse Fourier transform of the filtered component, represented by $I_{f_m}(t)$ and $I_{2f_m}(t)$ respectively; and (4) computing $A_1(t)$ and $A_2(t)$ using the subsequent relation:

$$A_1(t) = \text{imag} \left\{ I_{f_m}(t) / e^{j(2\pi f_m t + \beta)} \right\} \quad (7)$$

$$A_2(t) = \text{real} \left\{ I_{2f_m}(t) / e^{j(4\pi f_m t + 2\beta)} \right\} \quad (8)$$

As for the modulation depth, a question which must be taken into account is the null points of the Bessel function. When $J_1(2a)$ or $J_2(2a)$ is zero, we can not use Eq. (6) to calculate the phase $\phi(t)$. As we all know, $J_1(2a)$ and $J_2(2a)$ are oscillating functions of parameter a , with a series of zero-crossings whose values are listed in Table 1. These values of a should be avoided when choosing the modulation depth of EOM.

Table 1. Values of a which null $J_1(2a)$ or $J_2(2a)$ (represented by X)

a (rad)	1.91	2.56	3.50	4.20	5.04	5.81	6.66	7.42	8.24
$J_1(2a)=0$	X		X		X		X		X
$J_2(2a)=0$		X		X		X		X	

As the modulation frequency is concerned, the occurrence of measurement error due to band overlapping in the frequency domain should be considered. $A_1(t)$ and $A_2(t)$ have instantaneous frequency $F = d\phi(t)/(2\pi dt)$ which is proportional to the speed of the external target. Therefore, the first harmonic and the second harmonic centered at f_m and $2f_m$ present a spectral width proportional to the maximum velocity of the external target. To avoid overlapping problems, $\phi(t)$ can only have spectral components F limit to $f_m/2$:

$$F \leq f_m / 2 \quad (9)$$

For example, if the external target has a motion $d = d_0 \sin(2\pi ft)$, then $\phi(t) = 4\pi [L + d] / \lambda$. The instantaneous frequency F of $A_1(t)$ and $A_2(t)$ is

$$F = d\phi(t)/(2\pi dt) = 4\pi f d_0 \cos(2\pi ft) / \lambda \quad (10)$$

In order to satisfy the relationship in Eq. (9) all the time, the following relation should be satisfied:

$$F_{\max} = 4\pi f d_0 / \lambda \leq f_m / 2 \quad f_m \geq 8\pi f d_0 / \lambda \quad (11)$$

From Eq. (11) we can see that the minimum modulation frequency needed to demodulate the phase is directly proportional to the product of the amplitude and the frequency of the external target. So the measurement range of the system has no theoretical limit if the EOM has an enough high modulation frequency.

The phase ϕ obtained using the demodulation technique proposed is wrapped within the region of $-\pi/2$ and $\pi/2$. After a phase unwrapping process and following the relationship between the phase ϕ and the length of the external cavity, the movement of the external target can be reconstructed.

Assuming that the external target move at a sinusoidal form with amplitude $1\mu m$ and frequency 20HZ, the phase retrieved process is simulated in Fig. 2. The modulation depth of EOM is 1.1rad. The modulation frequency is 2KHZ. The output intensity of the laser is 1mW in the absence of feedback and the fringe visibility m is 0.08. The phase change due to the motion of the external target is demonstrated in Fig. 2(a). The modulated interference signal is shown in Fig. 2(b). The Fourier spectra of the SMI signal is shown in Fig. 2(c). Following the phase calculation steps, the phase is demodulated as in Fig. 2(d). After an unwrapping process,

the continuous phase is obtained as in Fig. 2(e). The phase retrieved error due to calculation is shown in Fig. 2(f). The max error is $2.5 \times 10^{-13} \text{ rad}$ in Fig. 2(f) and the standard deviation is $6.3 \times 10^{-14} \text{ rad}$.

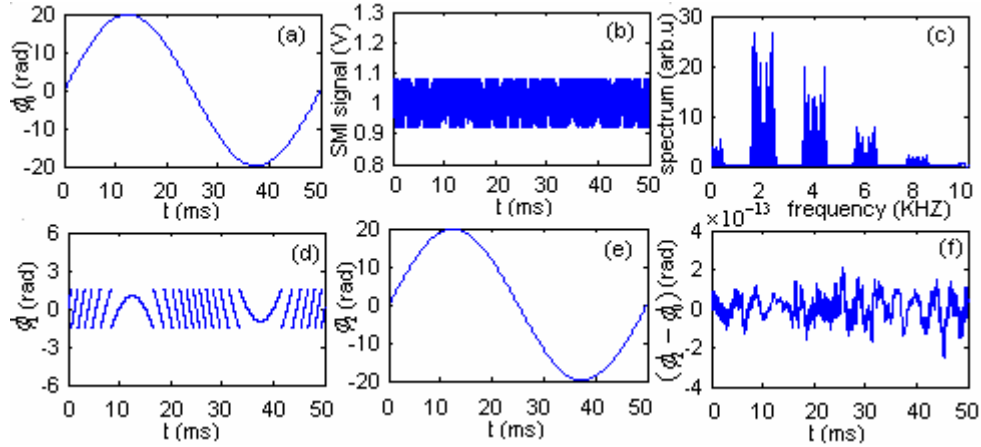


Fig. 2. (a) Simulated phase change due to the motion of the external target. (b) Simulated modulated interference signal. (c) Fourier spectra of the interference signal. (d) Calculated phase (wrapping). (e) Retrieved phase (unwrapped). (f) Phase retrieved error.

When the effect of multiple reflections can not be neglected completely, the additional terms in Eq. (1) (i.e., $j = 1, 2, \dots$) will cause phase retrieved error. Since the interferometer is restricted in a low feedback regime during measurement, we only consider the phase retrieved error caused by the second feedback in the external cavity (i.e., error caused by additional term $j = 1$). Figure 3 shows the phase retrieved error due to the second feedback in the external cavity corresponding to Fig. 2 in the condition of $m/\eta = 0.5$. The maximum error is 0.05 rad and the standard deviation is 0.03 rad. Figure 4 shows the maximum error and the standard deviation caused by $j = 1$ with respect to m in the condition of $m/\eta = 0.5$. Other simulation parameters are the same as in Fig. 2.

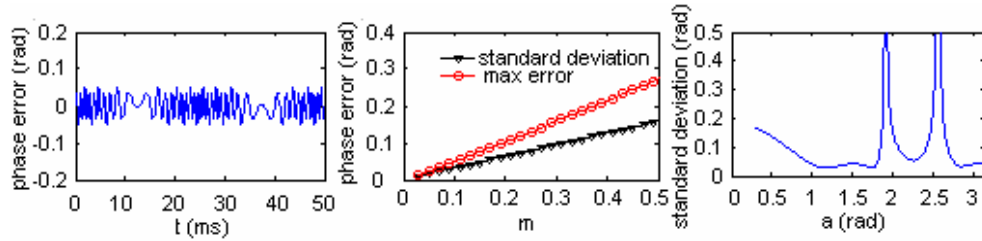


Fig. 3. Phase retrieved error due to the second feedback.

Fig. 4. Error caused by second feedback with respect to m .

Fig. 5. Standard deviation caused by second feedback versus the modulation depth a .

For two reflections in the external cavity, the modulated interference signal is given by

$$I(t) = I_0 \{1 + m \cos[\phi(t) + 2a \sin(2\pi f_m t + \beta)] - m\eta \cos^2[\phi(t) + 2a \sin(2\pi f_m t + \beta)]\} \quad (12)$$

Then the demodulated phase $\phi(t)_{j=0,1}$ is related to the actual phase $\phi(t)$ by

$$\tan(\phi(t)_{j=0,1}) = \frac{A_1(t)}{A_2(t)} \cdot \frac{J_2(2a)}{J_1(2a)} = \frac{1 - \eta \cos \phi(t) \frac{J_1(4a)}{J_1(2a)}}{1 - \eta \cos \phi(t) \frac{J_2(4a)}{J_2(2a)} + \frac{\eta}{2 \cos \phi(t)} \frac{J_2(4a)}{J_2(2a)}} \tan \phi(t) \quad (13)$$

From Eq. (13) we can see that the modulation depth of the EOM influence the phase retrieved error due to second feedback in the external cavity. So the appropriate modulation depth a can be selected to decrease the influence of the multiple reflections. Here the modulation depth is limited in the region of $a < \pi$ considering the operating characteristic of the EOM we used. Figure 5 shows the standard deviation caused by the second feedback in the external cavity versus modulation depth a in the condition of $m/\eta = 0.5$. Other simulation parameters are the same as in Fig. 2. It is obvious that the appropriate range of the modulation depth is $a \in [1.1rad, 1.8rad] \cup [2.8rad, 3.14rad]$. For simulation of other parameters (not reported here for brevity), the same range can be obtained.

4. Experimental results

Experiments have been done to confirm the validity of the sinusoidal phase modulating self-mixing interferometer and the phase demodulation method. In our experiment the first rising edge of TTL level from the signal generator which drives the EOM driver is introduced to the A/D card as the trigger of data acquisition. Then a sinusoidal phase modulation with the initial phase $\pi/2$ can be obtained.

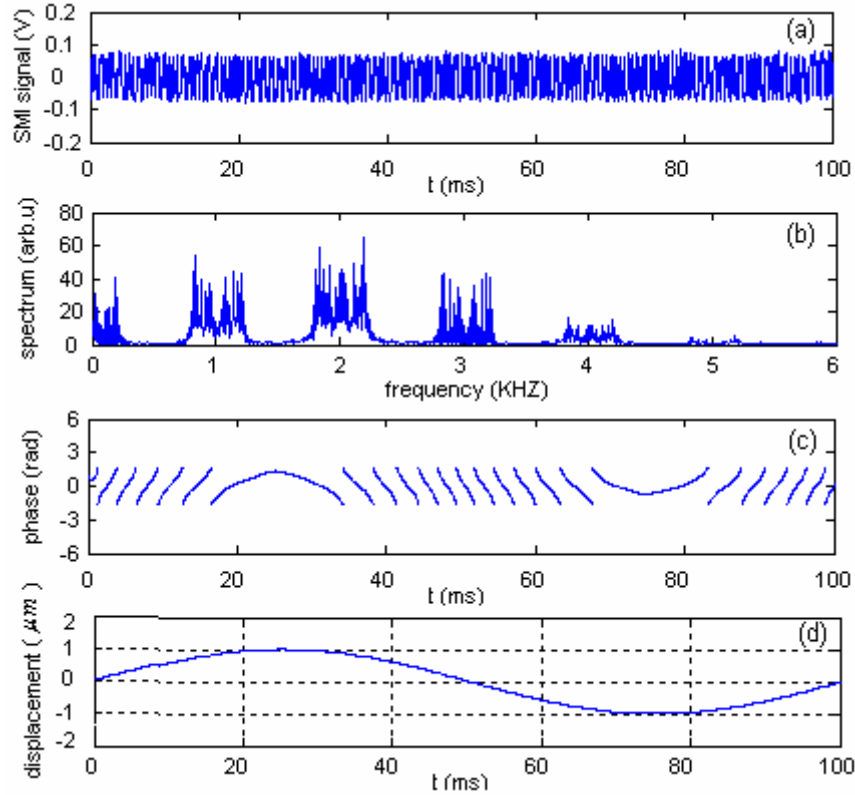


Fig. 6. (a) The obtained SMI signal. (b) Fourier spectra of the SMI signal. (c) Extracted phase (wrapping). (d) Displacement reconstruction result.

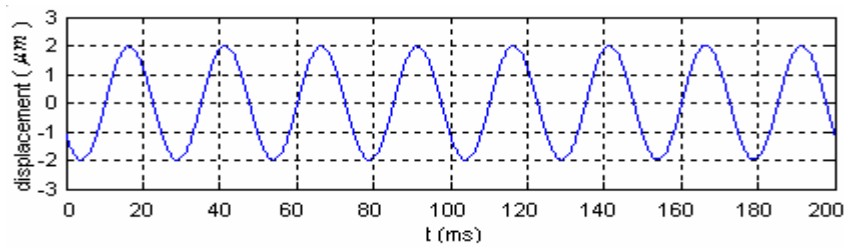


Fig. 7. Displacement reconstruction result of PZT with frequency 40HZ and amplitude of $4\mu\text{m}$ (peak to peak).

First, the PZT is controlled to move at a sinusoidal form with frequency 10HZ and amplitude $2\mu\text{m}$ (peak to peak). The modulation frequency is 1KHZ and the modulation depth is 1.2rad. The sampling rate of the A/D card is 50KHZ. Figure 6(a) is the interference signal obtained by A/D card. Figure 6(b) is the Fourier spectra of the detected signal in which the first harmonic component centered at 1KHZ and the second harmonic component centered at 2KHZ. Following the phase extraction steps, the phase is retrieved as in Fig. 6(c). After unwrapping the phase and using the relationship between the phase ϕ and the length of the external cavity, the movement of PZT is reconstructed as in Fig. 6(d). In displacement measurement, only the relative value of the two positions is important. So, we examine the peak-to-peak amplitude in Fig. 6(d) and get the displacement measurement accuracy. The peak-to-peak amplitude of the reconstructed waveform in Fig. 6(d) is $2.002\mu\text{m}$. Second the PZT is controlled to move at a sinusoidal form with frequency 40HZ and amplitude $4\mu\text{m}$ (peak to peak). The modulation frequency is 6KHZ and the modulation depth is 1.2rad. The sampling rate of A/D card is 100KHZ. The reconstruction result is in Fig. 7 and the max error for displacement measurement is 7nm.

5. Conclusion

The numerical simulation and experimental results show that the proposed new method can effectively demodulate the phase of the interference signal with high accuracy. The combination of modulation and demodulation decreases the sensitivity of the instrument to fluctuations of the laser power and the noise induced by environment. Since the minimum modulation frequency needed to demodulate the phase is directly proportional to the product of the amplitude and the frequency of the external target, the measurement range of the setup mainly depends on the maximum operating frequency of EOM and the maximum sampling rate of A/D converter. Considering that EOM can operate at a frequency up to 100MHZ, the system presented in this paper has a larger measurement range regarding the frequency and the amplitude of the motion of the measured object than the traditional SMI. In our experiments, we only reconstructed the movement of PZT with amplitude (peak to peak) up to $8\mu\text{m}$ and frequency up to 60HZ due to the limitation of the PZT used and a displacement measurement precision of $<10\text{ nm}$ can be obtained. So the sinusoidal phase modulating SMI offers both the resolution and measurement range increase in the self-mixing displacement sensor. Besides the application of displacement measurement presented in this paper, the sinusoidal phase modulating SMI can also be used to microvibration measurement and surface profile measurement. The related works will be reported in the future.

Acknowledgments

This work was supported by the National Natural Science Foundation of China, No. 50375074.